BIOCHEMISTRY
including biophysical chemistry & molecular biology

Article

pubs.acs.org/biochemistry

Metal-Ion Dependent Catalytic Properties of *Sulfolobus solfataricus* Class II α-Mannosidase

Jonas Willum Nielsen,[†,‡] Nina Rødtness Poulsen,[‡] Anna Johnsson,[†] Jakob Rahr Winther,[‡] S. L. S. Stipp,[†] and Martin Willemoës*[,‡]

[†]Nano-Science Center, Department of Chemistry, University of Copenhagen, Universitetsparken 5, DK-2300 Copenhagen Ø, Denmark

[‡]Department of Biology, University of Copenhagen, Ole Maaløes vej 5, DK-2200 Copenhagen N, Denmark

ABSTRACT: The active site for the family GH38 class II α-mannosidase is constituted in part by a divalent metal ion, mostly Zn^{2+}, as revealed in the crystal structures of enzymes from both animal and bacterial sources. The metal ion coordinates to the bound substrate and side chains of conserved amino acid residues. Recently, evidence has accumulated that class II α-mannosidase is active in complex with a range of divalent metal ions. In the present work, with employment of the class II α-mannosidase, ManA, from the hyperthermophilic archaeon *Sulfolobus solfataricus*, we explored the influence of the divalent metal ion on the associated steady-state kinetic parameters, K_M and k_{cat}, for various substrates. With *p*-nitrophenyl-α-D-mannoside as a substrate, the enzyme showed activity in the presence of Co^{2+}, Cd^{2+}, Mn^{2+}, and Zn^{2+}, whereas Ni^{2+} and Cu^{2+} were inhibitory and nonactivating. Co^{2+} was the preferred metal ion, with a k_{cat}/K_M value of about 120 mM^{-1} s^{-1}, 6 times higher than that with Cd^{2+} and Zn^{2+} and 10 times higher than that with Mn^{2+}. With α-1,2-, α-1,3-, α-1,4-, or α-1,6-mannobiose as a substrate, Co^{2+} was the only metal ion promoting hydrolysis of all substrates; however, Mn^{2+}, Cd^{2+}, and Zn^{2+} could substitute to a varying extent. A change in the divalent metal ion generally affected the K_M for the hydrolysis of *p*-nitrophenyl-α-D-mannoside; however, changes in both k_{cat} and K_M for the hydrolysis of α-mannobioses were observed, along with changing preferences for the glycosidic linkage. Finally, it was found that the metal ion and substrate bind in that order via a steady-state, ordered, sequential mechanism.

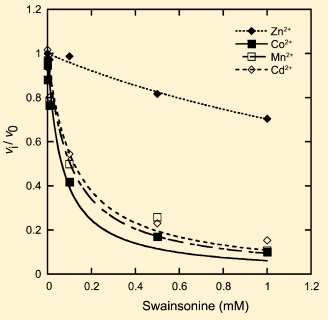

Class II α-mannosidases are exohydrolases that belong to glycoside hydrolase family 38 and hydrolyze mannosidic linkages via the retaining mechanism.[1] Extensive reviews of the physiological role and activity profiles of class II α-mannosidase are available from the literature.[2,3] The specificities of the enzymes range from cleaving only α-1,3 and α-1,6 glycosidic bonds to include α-1,2 and α-1,4 linkages as well.[4,5] In eukaryotes, class II α-mannosidase resides in the Golgi apparatus, the cytosol, and the lysosomes, where the enzyme participates in processing the N-glycosylated proteins as well as in catabolism of glycans originating from, for example, unfolded or endocytosed proteins.[2] The function of class II α-mannosidase in Bacteria and Archaea is more obscure, but most likely the enzyme serves similar functions, which is supported by the discovery of protein glycosylation in prokaryotes.[6,7] In the crenarchaeon *Sulfolobus solfataricus,* a recent report provides evidence for a likely role of class II α-mannosidase, ManA, in the processing of an extracellular polymeric substance known as EPS and maybe also in the processing of *N*-glycans of proteins located in the S-layer.[8] ManA has previously been characterized with respect to both physical properties and substrate specificity.[9]

The class II α-mannosidase is fully dependent on a divalent metal ion that participates in the binding of the mannosyl in site −1, preceding the scissile bond of the substrate.[10] Structural analysis of ligand complexes of the enzyme from *Streptococcus pyogenes*[11] suggested that the metal-ion complex distorts the mannosyl to be cleaved off and, in this way, facilitates transition-state formation. Likewise, identification occurred via structural analysis of four highly conserved residues, two histidines and two aspartates, that complex the metal ion in addition to a water molecule. Thus, an overall square pyramidal coordination sphere surrounds the divalent metal ion.[5,11] One of the aspartates complexing the metal ion is also suggested to be the catalytic nucleophile.[11,12] Upon substrate binding (Figure 1), the protein ligands remain bound to the metal ion; the water molecule ligand is replaced by the 2-hydroxyl of the bound mannosyl, and an additional ligand bond is formed with the 3-hydroxyl,[5,10,11] resulting in a complete octahedral coordination sphere for the metal ion.[5,11] In all published crystal structures of the enzyme, Zn^{2+} is located in the active site.[5,11−13] However, promiscuity in divalent metal-ion activation has been reported.[4,9,14] An example is the enzyme from *Thermotoga maritima* which shows maximum activity when complexed with Co^{2+} or Cd^{2+} but is also activated by Fe^{2+}, Cr^{2+}, Mn^{2+}, and Zn^{2+}.[4]

The relation between kinetic properties of ManA and specific properties of complex formation of the bound metal ion could

Received: August 14, 2012
Revised: September 18, 2012
Published: September 18, 2012

   dx.doi.org/10.1021/bi301096a | *Biochemistry* 2012, 51, 8039−8046

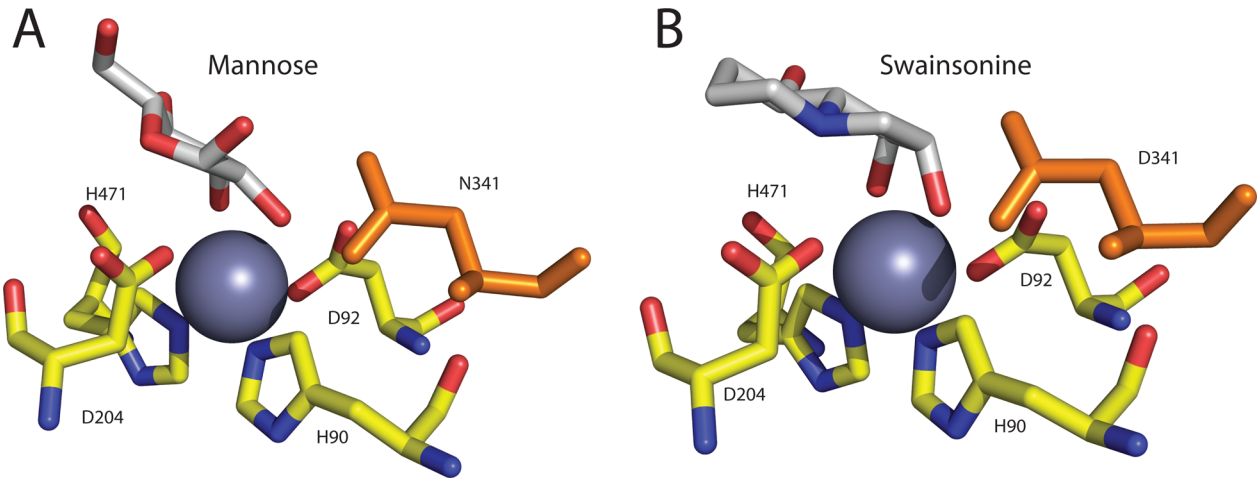

Figure 1. Structure of the active site of Golgi class II mannosidase from *Drosophila melanogaster* in complex with (A) mannose and (B) swainsonine. The amino acid residues involved in metal-ion binding are labeled by the one-letter code and numbered accordingly: H90, D92, D204, and H471. The 2-hydroxyl and 3-hydroxyl of mannose and swainsonine, respectively, also complex the bound Zn^{2+} ion. D204 is the proposed nucleophile. The acid/base D341 (orange) not interacting with the bound metal ion. The data used for the drawings are PDB entries 3BUP and 3BLB, respectively. The figure was generated using PyMol.

serve as an interesting platform for not only studying metal-ion binding sites and their interaction with substrates but also engineering of metal-ion binding sites with affinity for metal ions other than those bound by the wild-type ManA.

Typically, the divalent metal-ion preference of class II α-mannosidases has been evaluated by less informative specific activity measurements and not a full kinetic analysis. Ideally, the latter provides the kinetic parameters, K_M and k_{cat}, for the substrate, but at least k_{cat}/K_M is revealed, representing a kinetic value much stronger than the specific activities where the degree of saturation of the enzyme is unknown. Furthermore, until now nothing has been reported about the kinetic mechanism of metal-ion binding for this class of enzymes or the influence of changing the metal ion in the specific inhibition by swainsonine. To elucidate the influence of the nature of the divalent metal ion on the kinetic parameters of class II α-mannosidase, the present work describes a kinetic analysis of the enzyme from *S. solfataricus*, ManA,[9] in complex with a range of divalent metal ions.

EXPERIMENTAL PROCEDURES

Materials. All chemicals were acquired from Sigma Aldrich except for α-mannobioses, which came from Carbosynth.

Cloning and Expression of ManA from *S. solfataricus*. A PCR product encoding ManA from *S. solfataricus* strain P2 was obtained from chromosomal DNA using the following oligo-deoxyribonucleotides as primers: S.s.5.2ManA, GGGAA-TTCCATATGAGAAACATAAACGAGCTTGAGGCG; S.s.3.2manA, CGCGGATCCCTAACCCCTCACACTTATT-GTGAGGATATCCC. The restriction endonuclease sites, NdeI and BamHI, incorporated in the above primers, indicated by underlining, were used to clone the PCR fragment into the same restriction endonuclease sites of the expression vector pET11a, resulting in the plasmid pJWN01.

Escherichia coli strain BL21 (DE3) transformed with pRARE (Rosetta) and pJWN01 was grown with vigorous agitation in 2 L of a phosphate-buffered salt medium supplemented with tryptone and yeast extract, as described previously,[15] with the addition of chloramphenicol (50 μg/mL) and ampicillin (500 μg/mL) to maintain the plasmids. Expression was induced with 1 mM IPTG at an OD_{436} of 8−10 and continued overnight. Cells were harvested by centrifugation, washed twice in 50 mM potassium phosphate (pH 7.5), and resuspended in 130 mL of 50 mM Tris-HCl (pH 8.0). Cells were disrupted by sonication, and insoluble matter was removed by centrifugation for 20 min at 13000 rpm in a Sorvall rotor SS34.

A large fraction (>90%) of the produced ManA was insoluble and remained in the pellet with cell debris. Streptomycin sulfate was added to the cell extract to a final concentration of 1%, and the precipitate was centrifuged as described above. The supernatant was heated to 80 °C for 20 min before repeating centrifugation as described above. The supernatant was made 80% saturated with ammonium sulfate, and the pellet collected by centrifugation, as described above, was dissolved in 6.5 mL of 50 mM Tris-HCl (pH 8.0) and dialyzed against the same buffer. The dialysate was then loaded on a 5 mL HiTrap (GE Healthcare) anion exchange column equilibrated with 50 mM Tris-HCl (pH 8.0) and eluted by a NaCl gradient from 0 to 0.5 M. Fractions were analyzed by SDS−PAGE, and those containing pure α-mannosidase were pooled and made 80% saturated with ammonium sulfate. ManA was collected by centrifugation as described above, redissolved in 3 mL of 50 mM Tris-HCl (pH 8.0), and dialyzed through two changes of 500 mL of the same buffer. The dialyzed protein was stored at 4 °C. Two milliliter preparations of apo-ManA, 0.45 mg/mL, were prepared by incubation in 50 mM Tris-HCl (pH 8.0) and 5 mM EDTA at 70 °C for 1 h. The EDTA-treated ManA was twice subjected to dialysis in 200 mL of 50 mM Tris-HCl (pH 8.0) and 5 mM EDTA, followed by three stages of dialysis against 200 mL of 50 mM Tris-HCl (pH 8.0). The apoenzyme was stored at 4 °C.

Enzyme Assays and Kinetic Analysis. All enzyme assays were performed at 70 °C in 50 mM sodium acetate (pH 5.0). The concentration of the divalent metal ion was 0.1 mM, if not stated otherwise. Initial rates were determined at least twice, with ranges of enzyme concentrations dependent on the substrate: 6−60 nM in the presence of pNP-mannoside and 0.17−0.68 μM in the presence of α-mannobioses. The pNP-mannoside dependent reaction was terminated by adding 200 μL of 1 M sodium carbonate to 100 μL of an assay incubation

dx.doi.org/10.1021/bi301096a | *Biochemistry* 2012, 51, 8039−8046

and subsequent cooling on ice before the absorbance was read at 405 nm. As previously reported for pNP-mannoside, a nonenzymatic hydrolysis was observed in the presence of high Mn^{2+} concentrations.[4] However, when Mn^{2+} concentrations were kept at 100 μM or below, this reaction was undetectable within the incubation times of the enzyme assay. The α-mannobiose dependent reaction was accessed using a colorimetric assay for the formation of the reducing ends.[16] From a 100 μL incubation, aliquots of 15 μL were removed at various time points over a period of 20 min and quenched by the addition of a cooled colorimetric assay solution. Because the background signal from the α-mannobioses was quite high, the final colorimetric assay volume was adjusted proportionally with the reagent and water to dilute the reducing end content, in order to maintain the combined signal from the background and the reaction within the detection limits. The quenched reaction mixtures were incubated at 70 °C for 30 min and put on ice, and then the absorbance at 562 nm was determined.

Equation 1 was fitted to the data from measuring the initial rates at the various substrate concentrations. Equation 2 replaced eq 1 when a linear correlation between initial rates and substrate concentration persisted up the highest achievable substrate concentration.

$$v = \frac{k_{cat}[S]}{K_M + [S]} \quad (1)$$

$$v = \frac{k_{cat}}{K_M}[S] \quad (2)$$

where v represents the initial rate; k_{cat} is the maximum rate at infinitely high concentrations of the substrate, S, and K_M is the Michaelis–Menten constant.

Equation 3 was used to fit data from initial rates obtained in the presence of varying concentrations of inhibitor. Equation 4 was used to correct eq 3 for the influence of substrate concentration on inhibition. Equation 5 is the equation for competitive inhibition. Equation 6 is the equation for uncompetitive inhibition:

$$\frac{v_i}{v_0} = \frac{1}{1 + \frac{[I]}{K_i^{app}}} \quad (3)$$

$$K_i = \frac{K_i^{app}}{1 + \frac{[S]}{K_M}} \quad (4)$$

$$v = \frac{k_{cat}^{app}[S]}{K_M\left(1 + \frac{[I]}{K_{is}}\right) + [S]} \quad (5)$$

$$v = \frac{k_{cat}^{app}[S]}{K_M + [S]\left(1 + \frac{[I]}{K_{ii}}\right)} \quad (6)$$

where v_0 and v_i represent the initial rates determined in the absence and presence of the inhibitor, I, respectively, with the apparent inhibition constant, K_i^{app}, and the substrate independent inhibition constant, K_i. k_{cat}^{app} is the apparent maximum rate obtained by varying either the substrate or the divalent metal-ion concentration in the presence of a fixed, unsaturated concentration of the other. K_{is} and K_{ii} represent the inhibition constants for competitive and uncompetitive inhibition, respectively. Equation 7 is the equation for a two substrate, steady-state sequential reaction mechanism.

$$v = (k_{cat}[A][B])/(K_{ia}K_b + K_a[B] + K_b[A] + [A][B]) \quad (7)$$

where [A] and [B] represent the two substrates with the Michaelis–Menten constants, K_a and K_b, respectively. K_{ia} denotes the dissociation constant for substrate A.

The initial rate data were analyzed by nonlinear regression using either Ultrafit 3.0 (Biosoft) or Kaleidagraph 4.0 (Synergy Software). The presentations of linearized initial velocity data are based on global fits using nonlinear regression. All kinetic parameters are given with the standard error of the fit.

RESULTS

Enzyme Purification. The *S. solfataricus* ManA was purified to homogeneity as described in Experimental Procedures. The yield of soluble ManA was 4–5 mg from a 2 L cell culture; however, large quantities were discarded as insoluble precipitates. Various attempts to refold this insoluble fraction of ManA were unsuccessful.

Steady-State Kinetics of Substrate Saturation for ManA Substituted with Various Divalent Metal Ions. Initial activity measurements with pNP-mannoside as a substrate were performed with the inactive apoenzyme in the presence of one of the divalent metal ions at 100 μM: Zn^{2+}, Mn^{2+}, Co^{2+}, Cd^{2+}, Mg^{2+}, Ni^{2+}, or Cu^{2+}, among which Zn^{2+}, Mn^{2+}, Co^{2+}, and Cd^{2+} activated the enzyme. The kinetic parameters from steady-state kinetic analysis of pNP-mannoside saturation of the active ManA–metal-ion complexes are shown in Table 1. When substituted with Co^{2+}, ManA had a k_{cat}/K_M value for the substrate that was 6–10 times higher than that found for the enzyme harboring Zn^{2+}, Cd^{2+}, or Mn^{2+} (Table 1). This property of the Co^{2+}-substituted enzyme mainly resided with a comparatively low substrate K_M. ManA in complex with Zn^{2+}, Cd^{2+}, or Mn^{2+} showed somewhat similar k_{cat}/K_M values for the substrate (Table 1). However, Zn^{2+}- and Cd^{2+}-substituted ManA had a higher k_{cat} value with a slight increase in K_M for pNP-mannoside compared with that of the Mn^{2+}-substituted enzyme (Table 1).

Table 1. Kinetic Parameters of pNP-Mannoside Hydrolysis by ManA in Complexes with Various Divalent Metal Ions[a]

metal ion	K_M (mM)	k_{cat} (s^{-1})	k_{cat}/K_M (mM^{-1} s^{-1})
–[b]	1.0 ± 0.1	10.5 ± 0.6	10.5
Co^{2+}	0.11 ± 0.02	12.5 ± 0.6	120
Zn^{2+}	0.65 ± 0.09	13.6 ± 0.5	21
Cd^{2+}	0.99 ± 0.15	16.1 ± 0.8	16
Mn^{2+}	0.39 ± 0.03	4.8 ± 0.1	12

[a]Details about assays are described in Experimental Procedures. Kinetic parameters were calculated using eq 1. [b]This is an untreated enzyme which has not been subjected to EDTA treatment (see Experimental Procedures) and with no externally added metal ion in the incubation assay.

Class II α-mannosidase is known to have a broad specificity toward the α-1,x linkages in their substrates, where x can be 2, 3, and 6.[4,12,14] Although the steady-state kinetics on pNP-mannoside readily revealed differences in the kinetic parameters of ManA depending on the metal-ion substitution (Table 1), there might be even more pronounced differences with α-mannobioses, constituting a more natural substrate for ManA.

dx.doi.org/10.1021/bi301096a | *Biochemistry* 2012, 51, 8039–8046

ManA was active on α-1,2-, α-1,3-, and α-1,6-mannobioses, as previously demonstrated.[9] In addition, α-1,4-mannobiose, which has not previously been tested, was also found to be a substrate. Table 2 lists the kinetic parameters obtained from steady-state kinetic analysis of ManA substituted with Zn^{2+}, Mn^{2+}, Co^{2+}, and Cd^{2+} on the different α-mannobioses. The k_{cat}/K_M values determined for mannobioses with the Co^{2+} enzyme were fairly constant regardless of whether α-1,2-, α-1,3-, or α-1,4-disaccharide was the substrate and was significantly lower on α-1,6-mannobiose (Table 2). Complexed with Zn^{2+}, Cd^{2+}, or Mn^{2+}, ManA was less active on α-mannobioses compared with ManA complexed with Co^{2+} (Table 2), consistent with the observations for pNP-mannoside (Table 1). One remarkable difference observed between the substrates, pNP-mannoside and α-mannobioses, was that Mn^{2+} was preferred over Zn^{2+} and Cd^{2+}, as evaluated from k_{cat}/K_M for α-1,2- and α-1,4-mannobiose (Table 2). In fact, Mn^{2+} was the only metal ion in addition to Co^{2+} that gave substrate K_M values low enough for a reliable determination of the individual kinetic parameters, k_{cat} and K_M (Table 2).

Although ManA displayed similar k_{cat}/K_M values on α-1,2-, α-1,3-, and α-1,4-mannobiose when Co^{2+} was the activating metal ion, the same was not found for ManA substituted with Mn^{2+}. Here, the k_{cat}/K_M value for α-1,3-mannobiose was about 5 times lower than those of α-1,2- and α-1,4-mannobiose (Table 2). The α-1,6-mannobiose was not a substrate for Mn^{2+}-, Cd^{2+}-, or Zn^{2+}-substituted ManA, at least not at the tested substrate concentrations (Table 2).

Table 2. Kinetic Parameters for Hydrolysis of α-Mannobioses by ManA in Complex with Various Metal Ions[a]

metal ion	α-mannobiose	K_M (mM)	k_{cat} (s^{-1})	k_{cat}/K_M (mM^{-1} s^{-1})
Co^{2+}	α-1,2-mannobiose	0.85 ± 0.07	5.5 ± 0.2	6.4
	α-1,3-mannobiose	1.16 ± 0.47	4.9 ± 0.6	4.2
	α-1,4-mannobiose	2.5 ± 0.3	10.4 ± 0.4	4.2
	α-1,6-mannobiose	2.0 ± 0.4	2.0 ± 0.2	1.0
Zn^{2+}	α-1,2-mannobiose	ND[b]	ND[b]	0.206 ± 0.008
	α-1,3-mannobiose	ND[b]	ND[b]	0.102 ± 0.005
	α-1,4-mannobiose	ND[b]	ND[b]	0.106 ± 0.005
	α-1,6-mannobiose	–[c]	–[c]	–[c]
Cd^{2+}	α-1,2-mannobiose	ND[b]	ND[b]	0.277 ± 0.007
	α-1,3-mannobiose	ND[b]	ND[b]	0.28 ± 0.05
	α-1,4-mannobiose	ND[b]	ND[b]	0.31 ± 0.01
	α-1,6-mannobiose	–[c]	–[c]	–[c]
Mn^{2+}	α-1,2-mannobiose	2.3 ± 0.3	3.1 ± 0.2	1.3
	α-1,3-mannobiose	ND[b]	ND[b]	0.185 ± 0.009
	α-1,4-mannobiose	2.0 ± 0.6	1.9 ± 0.2	0.95
	α-1,6-mannobiose	–[c]	–[c]	–[c]

[a]Experiments were performed as described in Experimental Procedures. Data were analyzed using eq 1, unless otherwise noted. [b]ND = not determined. In these data sets, the K_M was too high to be determined, and the k_{cat}/K_M value was calculated using eq 2. [c]No measurable activity.

Inhibition by Swainsonine of ManA Substituted with Various Divalent Metal Ions. Swainsonine is a competitive inhibitor of class II α-mannosidase.[4,5,11] Figure 2 shows the swainsonine inhibition of ManA substituted with Zn^{2+}, Mn^{2+}, Co^{2+}, and Cd^{2+}. From the inhibition constant, K_i^{app}, obtained from eq 3, the substrate concentration independent inhibition constant, K_i, was calculated using eq 4. The values of K_i and K_i^{app} for the individual experiments are given in the legend of Figure 2. K_i values in the micromolar range obtained in the present study are not uncommon for swainsonine inhibition of class II α-mannosidase.[11,14] However, the observation that ManA substituted with Zn^{2+} is considerably less sensitive to swainsonine compared with the Co^{2+}-, Cd^{2+}-, and Mn^{2+}-substituted enzyme is surprising because a previous work reports a K_i^{app} value of 0.2 mM, corresponding to a $K_i \approx 30$ μM, for the Zn^{2+}-substituted ManA.[9]

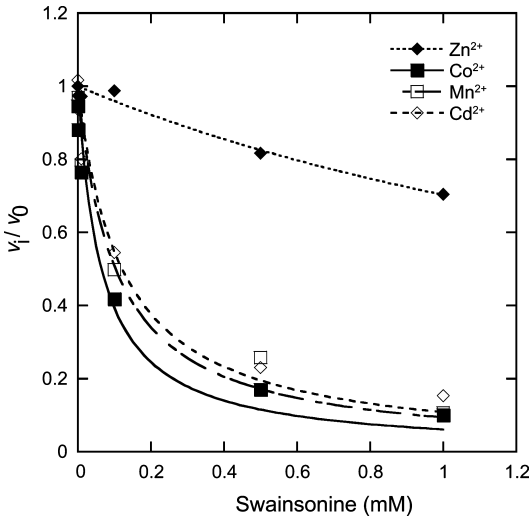

Figure 2. Inhibition of ManA hydrolysis of pNP-mannoside by swainsonine. The experiments were performed as described in Experimental Procedures. Initial rates are from experiments where the swainsonine concentration was varied at fixed concentrations of pNP-mannoside in the presence of the divalent metal ions as indicated. K_i^{app} and K_i were calculated using eqs 3 and 4: (■) Co^{2+}, 0.6 mM pNP-mannoside; K_i^{app} = 65 ± 16 μM; K_i = 10 μM; (□) Mn^{2+}, 0.5 mM pNP-mannoside; K_i^{app} = 104 ± 23 μM; K_i = 46 μM; (◇) Cd^{2+}, 5 mM pNP-mannoside; K_i^{app} = 120 ± 21 μM; K_i = 20 μM; (◆) Zn^{2+}, 0.6 mM pNP-mannoside; K_i^{app} = 2400 ± 170 μM; K_i = 1200 μM.

Steady-State Mechanism of Metal-Ion Binding to ManA. The apparent K_M values for Zn^{2+}, Cd^{2+}, and Co^{2+} for activation of ManA approached the enzyme concentration in the assay incubation. Therefore, Mn^{2+} with a somewhat higher K_M of about 0.6 μM was chosen as the activating metal ion in a kinetic analysis of the mechanism of substrate and metal-ion binding. The pattern of intersecting lines in Figure 3A is consistent with both an ordered and a random sequential mechanism.[17] To elucidate the mechanism in more detail, the inhibitor swainsonine was used as a substrate-binding analog, to distinguish between these two mechanisms. Consistent with swainsonine being a substrate-binding analog, we observed

dx.doi.org/10.1021/bi301096a | Biochemistry 2012, 51, 8039–8046

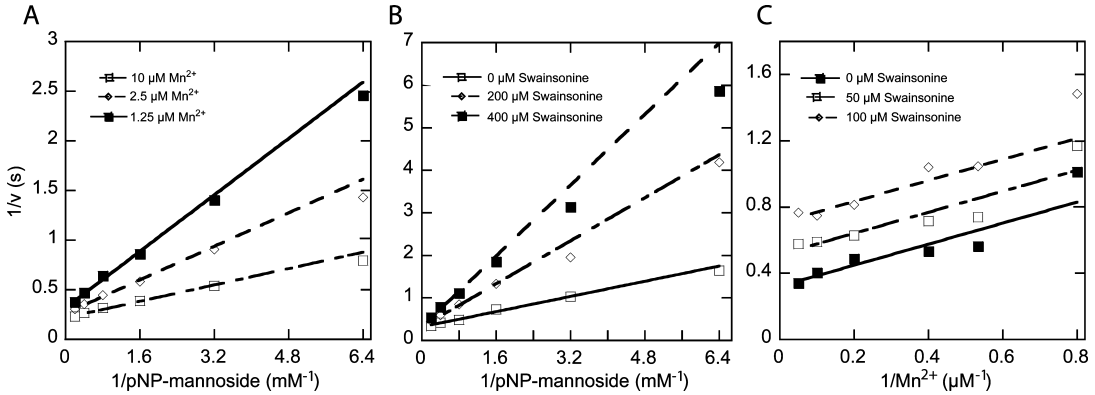

Figure 3. Binding mechanism of substrate and divalent metal ion to ManA. The experiments were performed as described in Experimental Procedures. (A) Double-reciprocal plots of initial rates at various concentrations of pNP-mannoside and $MnCl_2$ as indicated. Kinetic parameters calculated using eq 7 were $k_{cat} = 4.9 \pm 0.1\ s^{-1}$, $K_a = 0.70 \pm 0.1\ \mu M$, $K_{ia} = 5.4 \pm 1\ \mu M$, and $K_b = 0.33 \pm 0.04$ mM. (B) Double-reciprocal plots of initial rates at various concentrations of pNP-mannoside in the presence of 1.25 μM $MnCl_2$ and swainsonine, as indicated. Kinetic parameters calculated using eq 5 were $k_{cat}^{app} = 3.1 \pm 0.13\ s^{-1}$, $K_M = 0.70 \pm 0.090$ mM, and $K_{is} = 0.11 \pm 0.014$ mM. (C) Double reciprocal plots of initial rates at increasing concentrations of $MnCl_2$ in the presence of 0.6 mM pNP-mannoside and swainsonine as indicated. Kinetic parameters calculated using eq 6 were $k_{cat}^{app} = 3.1 \pm 0.12\ s^{-1}$, $K_M = 0.70 \pm 0.090$ mM, and $K_{ii} = 0.083 \pm 0.0076$ mM.

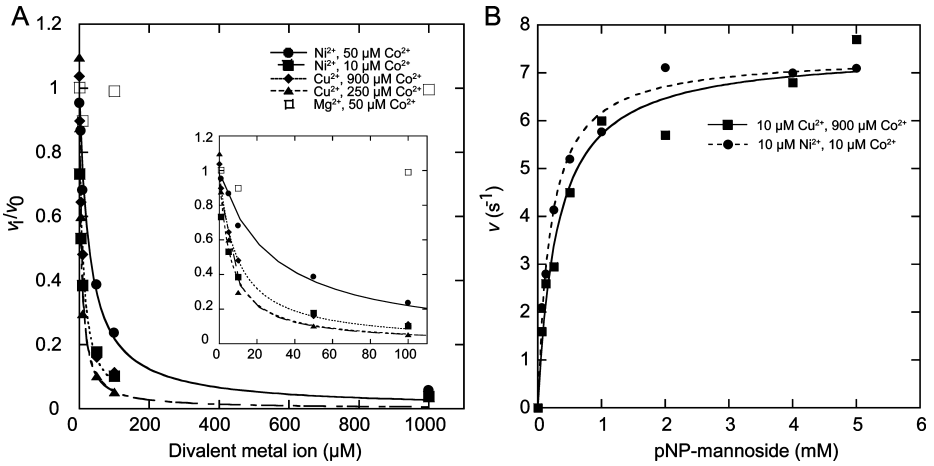

Figure 4. Inhibition of ManA by divalent metal ions. The experiments were performed as described in Experimental Procedures. (A) Initial rates of pNP-mannoside hydrolysis by ManA in the presence of various concentrations of Ni^{2+}, Cu^{2+}, or Mg^{2+}. The Co^{2+} concentration was varied as indicated, and pNP-mannoside was added to produce a concentration of 1 mM. Ni^{2+} was varied in the presence of a Co^{2+} concentration of (●) 50 μM or (■) 10 μM. Cu^{2+} was varied in the presence of a Co^{2+} concentration of (▲) 250 μM or (◆) 900 μM. Mg^{2+} was varied in the presence of a Co^{2+} concentration of (□) 50 μM. (B) Saturation curves of pNP-mannoside hydrolysis by ManA in the presence of (●) 10 μM Co^{2+} and 10 μM Ni^{2+} or (■) 900 μM Co^{2+} and 10 μM Cu^{2+}. Cu^{2+} and Ni^{2+} were added to a concentration resulting in about 50% inhibition. K_i^{app} values calculated from eq 3, corresponding to the shown curves and obtained as described in Experimental Procedures, were (●) 28 ± 2, (■) 5.7 ± 1, (▲) 5.9 ± 1, and (◆) 9.4 ± 0.6 μM.

competitive inhibition by swainsonine of pNP-mannoside saturation of ManA (Figure 3B). However, the diagnostic experiment shown in Figure 3C revealed uncompetitive inhibition of Mn^{2+} saturation by swainsonine when the metal ion was varied at different fixed concentrations of the inhibitor. The combined pattern of substrate saturation and swainsonine inhibition observed in Figure 3 is unique for a steady-state ordered mechanism in which the metal ion is bound prior to the binding of the substrate.[18] The kinetic parameters calculated from the experiments shown in Figure 3 are listed in the legend.

Metal-Ion Inhibition of ManA. Although Ni^{2+}, Mg^{2+}, and Cu^{2+} did not activate the apoenzyme, this did not exclude the binding of these three metal ions to the active site. The results presented in Figure 4A, derived from experiments that varied these metal ions, demonstrate that both Ni^{2+} and Cu^{2+} inhibit ManA in the presence of Co^{2+}. Mg^{2+} did not inhibit ManA, even at concentrations up to 1 mM (Figure 4A). In agreement with Ni^{2+} and Cu^{2+} being inhibitory, these two metal ions did not appear to promote substrate inhibition at increasing pNP-mannoside concentrations (Figure 4B), as would be expected if ManA, complexed with either Ni^{2+} or Cu^{2+}, was able to bind pNP-mannoside to the active site.

■ DISCUSSION

There have been no thorough investigations on the influence exerted by the exchange of the divalent metal ion on the kinetic properties of class II α-mannosidase or the role a change of the metal ion plays in substrate specificity. Except for two studies on prokaryotic enzymes,[4,14] most reports are based on the effect of metal ions on enzymes where the intrinsic metal ion has not been removed prior to analysis. Most likely, such scenarios describe the properties of a mix of enzyme−metal-ion complexes. In the present work, we have overcome this

dx.doi.org/10.1021/bi301096a | Biochemistry 2012, 51, 8039−8046

problem by developing a protocol for removing the divalent metal ion as a measure of the decrease in ManA activity to background levels and which upon addition of metal ion could be fully restored.

The relatively high k_{cat} values observed, in general, for pNP-mannoside compared to those of the α-mannobioses (Tables 1 and 2), as well as the variations in the k_{cat} value on the various α-mannobioses, point to the cleavage of the glycosidic bond of α-mannobioses as the rate-limiting step in substrate turnover, not uncommon for glycoside hydrolases.[19,20] The Co^{2+}-substituted ManA appears to be the kinetically superior metal-ion−enzyme complex based on the kinetics of both hydrolysis of pNP-mannoside and α-mannobioses (Tables 1 and 2). The fairly similar k_{cat}/K_M values for pNP-mannoside of ManA in the presence of Zn^{2+}, Cd^{2+}, and Mn^{2+} (Table 1) imply that the metal ion is mainly involved in substrate binding. Thus, a decrease in the substrate K_M by complex formation between the substrate and the divalent metal ion, resulting in a tight ground-state complex, would cause the activation energy for the transition-state formation to increase with a concomitant decrease in the k_{cat} value. The Co^{2+}-substituted ManA evidently stands out by maintaining a high k_{cat} value despite a low substrate K_M value (Table 1). This latter result represents a unique case for the investigated divalent metal ions where the kinetic parameters point to a stabilization of both the ground state complex and the transition state formed between Co^{2+} and substrate in the active site.

The kinetic analysis of α-mannobiose hydrolysis was, in many of the combinations of ManA and divalent metal ions, hampered by a K_M value for the dissacharide overly high to be measured accurately with the used assay technique. However, on the basis of the k_{cat}/K_M values, the trends for the influence of the divalent metal ions on α-mannobiose kinetics (Table 2) are similar to that of pNP-mannoside (Table 1). Also with mannobioses, ManA substituted with Co^{2+} remained the kinetically superior metal−enzyme complex (Table 2), and the Mn^{2+}-substituted enzyme maintained relatively low values of both substrate K_M and k_{cat} values, at least on α-1,2- and α-1,4-mannobiose. Conversely, ManA in complex with Cd^{2+} or Zn^{2+} showed k_{cat}/K_M values for α-1,2- and α-1,4-mannobiose that were much lower than those for the Mn^{2+} enzyme (Table 2), a result that clearly deviated from the results of pNP-mannoside (Table 1).

The impact of changing the divalent metal ion on the kinetic parameters for the substrate appears not to be uniformly applied to all substrates. This is demonstrated by the k_{cat}/K_M value for the Mn^{2+}−enzyme complex when α-1,3-mannobiose is the substrate compared to the k_{cat}/K_M values for α-1,2- and α-1,4-mannobiose (Table 2). In general, activity of class II α-mannosidase on α-1,4-mannobiose is not reported in the literature, because either the activity has not been tested or it has not been considered relevant with respect to the task of demannosylating N-glycans. However, a couple of studies on enzymes from prokaryotes, *Picrophilus torridus*[14] and *T. maritima*,[4] report on this activity.

Many enzymes require a metal ion in order to function, and there are several examples of metal-ion binding enzymes displaying metal-ion promiscuity.[21−24] In rare cases, non-native metal ions may even make a more efficient enzyme.[21,23] In this context, it is important to note that different divalent metal ions show certain trends with respect to the coordination number and preferred side-chain ligands,[25,26] and theories such as the Irving−Williams series and the Pearson acid-base concept can assist in understanding the behavior of enzymes substituted with different divalent metal ions. Two histidines and two aspartates, of which all are conserved in ManA, bind to the divalent metal ion in class II α-mannosidase. Additional ligands are the 2-hydroxyl and 3-hydroxyl of the substrate (Figure 1A), in agreement with a hexacoordinated, octahedral arrangement around the bound metal ion.[5,11] Co^{2+}, Zn^{2+}, Cd^{2+}, and Mn^{2+} are all capable of forming complexes with histidines and aspartates; Co^{2+} and Mn^{2+} predominantly form octahedral complexes in proteins, and Zn^{2+} predominantly forms tetrahedral complexes. However, Cd^{2+} can adopt either of the two coordinations.[25,26] Therefore, it is not unlikely that Co^{2+} and to some extent Mn^{2+} when complexed in the active site of ManA promote a more efficient enzyme because of their preference for the octahedral conformation. Previous investigations on class II α-mannosidase from *S. pyogenes*[11] and bovine[12] have implied that the metal ion is involved both in substrate binding and in distortion toward the transition state, functions that can explain the observed variations in the k_{cat} and K_M values for the substrate (Tables 1 and 2). For swainsonine inhibition, K_i values in the micromolar range obtained in the present study (Figure 2) are not uncommon for class II α-mannosidases,[11,14,27] although the result indicates a weaker inhibition than typically seen for class II mannosidases. For example, Golgi and lysosomal class II mannosidases are strongly inhibited by swainsonine with K_i values in the nanomolar range.[5,28] swainsonine inhibition of ManA substituted with Zn^{2+} was less potent than with Co^{2+}, Cd^{2+}, or Mn^{2+}, maybe because the latter three metal ions typically induce an octahedral conformation favoring the Swainsonine complex (Figure 1B).[5,11]

The sequential ordered mechanism (Figures 3 and 5) observed for the binding of divalent metal ion and substrate

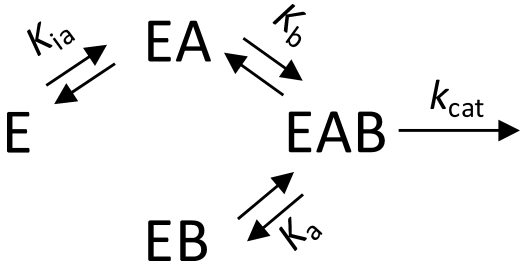

Figure 5. Scheme of the steady-state ordered sequential mechanism where the metal ion (A) binds and dissociates from the enzyme (E) at a rate on the same order of magnitude as the reaction. Another possibility is that an additional step (e.g., isomerization) immediately following the formation of EA, but prior to binding of substrate (B), occurs with a rate on the same order of magnitude as the catalytic rate.

to ManA, in that order, has been observed with other enzymes[24,29,30] and is perhaps not surprising, considering the role of the metal ion in substrate binding. In contrast to the rapid equilibrium mechanism generally observed for the binding of the metal ion to the enzyme,[24,29,30] the binding of Mn^{2+} to ManA is at a steady state. This indicates that the rates of binding and dissociation of Mn^{2+} from ManA, or a conformational change of the metal−enzyme complex prior to substrate binding following each round of catalysis, are on the same order of magnitude as the rate of the reaction. Figure 5 illustrates the steady-state ordered mechanism and the associated kinetic parameters. Interestingly, Cu^{2+} and Ni^{2+} are both strong inhibitors of ManA (Figure 4A), where Cu^{2+} stands out by having a K_i^{app} of 9 μM in the presence of 900 μM Co^{2+}.

dx.doi.org/10.1021/bi301096a | *Biochemistry* 2012, 51, 8039−8046

However, the absence of induced substrate inhibition (Figure 4B) in the presence of the inhibitory metal ions indicates that although ManA binds Cu^{2+} and Ni^{2+}, the binding of pNP-mannoside is not facilitated by these metal ions.

Although ManA has been shown to contain Zn^{2+} when purified from *S. solfataricus*,[9] we find that the zinc-bearing enzyme, although active, was very inefficient on all α-mannobioses. In addition, the inhibition by swainsonine, characteristic of class II α-mannosidase, was not as prominent with the Zn^{2+}-containing enzyme and much more efficient in the presence of the other activating divalent metal ions. Our observations, of course, do not necessarily warrant a suggestion that ManA is a Co^{2+} enzyme, but in the catalytic interplay among protein, metal ion, and substrate, Co^{2+} seems superior to all other tested divalent metal ions.

AUTHOR INFORMATION

Corresponding Author

*E-mail: willemoes@bio.ku.dk. Tel: +45 3532 2030.

Funding

This work was supported by the Danish National Advanced Technology Foundation (HTF), Maersk Oil and Gas A/S, and the University of Copenhagen through the Nano-Chalk Venture, as well as the Danish Council for Independent Research, Technology and Production Sciences.

Funding

This work was supported by the Danish National Advanced Technology Foundation (HTF), Maersk Oil and Gas A/S, and the University of Copenhagen through the Nano-Chalk Venture, as well as the Danish Council for Independent Research, Technology and Production Sciences. We sincerely thank Jesper Tholstrup Hansen for supplying the *S. solfataricus* strain P2 chromosomal DNA.

Notes

The authors declare no competing financial interest.

REFERENCES

(1) Howard, S., He, S., and Withers, S. G. (1998) Identification of the active site nucleophile in jack bean alpha-mannosidase using 5-fluoro-beta-L-gulosyl fluoride. *J. Biol. Chem. 273*, 2067−2072.

(2) Moremen, K. W., Ernst, B., Hart, G. W., and Sinaý, P. (2008) α-Mannosidases in Asparagine-Linked Oligosaccharide Processing and Catabolism. In *Carbohydrates in Chemistry and Biology*, pp 81−117, Wiley-VCH Verlag GmbH, Weinheim, Germany.

(3) Herscovics, A. (1999) Importance of glycosidases in mammalian glycoprotein biosynthesis. *Biochim. Biophys. Acta 1473*, 96−107.

(4) Nakajima, M., Imamura, H., Shoun, H., and Wakagi, T. (2003) Unique metal dependency of cytosolic α-mannosidase from *Thermotoga maritima*, a hyperthermophilic bacterium. *Arch. Biochem. Biophys. 415*, 87−93.

(5) van den Elsen, J. M., Kuntz, D. A., and Rose, D. R. (2001) Structure of Golgi alpha-mannosidase II: A target for inhibition of growth and metastasis of cancer cells. *EMBO J. 20*, 3008−3017.

(6) Abu-Qarn, M., Eichler, J., and Sharon, N. (2008) Not just for Eukarya anymore: Protein glycosylation in Bacteria and Archaea. *Curr. Opin. Struct. Biol. 18*, 544−550.

(7) Calo, D., Kaminski, L., and Eichler, J. (2010) Protein glycosylation in Archaea: Sweet and extreme. *Glycobiology 20*, 1065−1076.

(8) Koerdt, A., Jachlewski, S., Ghosh, A., Wingender, J., Siebers, B., and Albers, S. V. (2012) Complementation of *Sulfolobus solfataricus* PBL2025 with an alpha-mannosidase: Effects on surface attachment and biofilm formation. *Extremophiles 16*, 115−125.

(9) Cobucci-Ponzano, B., Conte, F., Strazzulli, A., Capasso, C., Fiume, I., Pocsfalvi, G., Rossi, M., and Moracci, M. (2010) The molecular characterization of a novel GH38 α-mannosidase from the crenarchaeon *Sulfolobus solfataricus* revealed its ability in de-mannosylating glycoproteins. *Biochimie 92*, 1895−1907.

(10) Shah, N., Kuntz, D. A., and Rose, D. R. (2008) Golgi alpha-mannosidase II cleaves two sugars sequentially in the same catalytic site. *Proc. Natl. Acad. Sci. U.S.A. 105*, 9570−9575.

(11) Suits, M. D. L., Zhu, Y., Taylor, E. J., Walton, J., Zechel, D. L., Gilbert, H. J., and Davies, G. J. (2010) Structure and Kinetic Investigation of *Streptococcus pyogenes* Family GH38 α-Mannosidase. *PLoS One 5*, e9006.

(12) Heikinheimo, P., Helland, R., Leiros, H. K., Leiros, I., Karlsen, S., Evjen, G., Ravelli, R., Schoehn, G., Ruigrok, R., Tollersrud, O. K., McSweeney, S., and Hough, E. (2003) The structure of bovine lysosomal alpha-mannosidase suggests a novel mechanism for low-pH activation. *J. Mol. Biol. 327*, 631−644.

(13) Numao, S., Kuntz, D. A., Withers, S. G., and Rose, D. R. (2003) Insights into the mechanism of *Drosophila melanogaster* Golgi alpha-mannosidase II through the structural analysis of covalent reaction intermediates. *J. Biol. Chem. 278*, 48074−48083.

(14) Angelov, A., Putyrski, M., and Liebl, W. (2006) Molecular and biochemical characterization of alpha-glucosidase and alpha-mannosidase and their clustered genes from the thermoacidophilic archaeon *Picrophilus torridus*. *J. Bacteriol. 188*, 7123−7131.

(15) Yung-Chi, C., and Prusoff, W. H. (1973) Relationship between the inhibition constant (KI) and the concentration of inhibitor which causes 50% inhibition (I50) of an enzymatic reaction. *Biochem. Pharmacol. 22*, 3099−3108.

(16) McFeeters, R. F. (1980) A manual method for reducing sugar determinations with 2,2′-bicinchoninate reagent. *Anal. Biochem. 103*, 302−306.

(17) Rudolph, F. B., and Fromm, H. J. (1979) Plotting methods for analyzing enzyme rate data. *Methods Enzymol. 63*, 138−159.

(18) Fromm, H. J. (1979) Use of competitive inhibitors to study substrate binding order. *Methods Enzymol. 63*, 467−486.

(19) Golden, E. B., and Byers, L. D. (2009) Methyl glucoside hydrolysis catalyzed by beta-glucosidase. *Biochim. Biophys. Acta 1794*, 1643−1647.

(20) Bravman, T., Zolotnitsky, G., Belakhov, V., Shoham, G., Henrissat, B., Baasov, T., and Shoham, Y. (2003) Detailed Kinetic Analysis of a Family 52 Glycoside Hydrolase: A β-Xylosidase from *Geobacillus stearothermophilus*. *Biochemistry 42*, 10528−10536.

(21) Kleifeld, O., Rulisek, L., Bogin, O., Frenkel, A., Havlas, Z., Burstein, Y., and Sagi, I. (2004) Higher metal-ligand coordination in the catalytic site of cobalt-substituted *Thermoanaerobacter brockii* alcohol dehydrogenase lowers the barrier for enzyme catalysis. *Biochemistry 43*, 7151−7161.

(22) Raasch, C., Streit, W., Schanzer, J., Bibel, M., Gosslar, U., and Liebl, W. (2000) *Thermotoga maritima* AglA, an extremely thermostable NAD^+-, Mn^{2+}-, and thiol-dependent α-glucosidase. *Extremophiles 4*, 189−200.

(23) Park, H. I., and Ming, L. J. (2002) Mechanistic studies of the astacin-like *Serratia* metalloendopeptidase serralysin: Highly active (>2000%) Co(II) and Cu(II) derivatives for further corroboration of a "metallotriad" mechanism. *J. Biol. Inorg. Chem. 7*, 600−610.

(24) Houston, L. L., and Graham, M. E. (1974) Divalent metal ion effects on a mutant histidinol phosphate phosphatase from *Salmonella typhimurium*. *Arch. Biochem. Biophys. 162*, 513−522.

(25) Rulisek, L., and Vondrasek, J. (1998) Coordination geometries of selected transition metal ions (Co^{2+}, Ni^{2+}, Cu^{2+}, Zn^{2+}, Cd^{2+}, and Hg^{2+}) in metalloproteins. *J. Inorg. Biochem. 71*, 115−127.

(26) Glusker, J. P., Katz, A. K., and Bock, C. W. (1999) Metal Ions in Biological Systems. *Rigaku J. 16*, 8−17.

(27) De Gasperi, R., Daniel, P. F., and Warren, C. D. (1992) A human lysosomal alpha-mannosidase specific for the core of complex glycans. *J. Biol. Chem. 267*, 9706−9712.

(28) Venkatesan, M., Kuntz, D. A., and Rose, D. R. (2009) Human lysosomal alpha-mannosidases exhibit different inhibition and metal binding properties. *Protein Sci. 18*, 2242−2251.

(29) Schutzbach, J. S., and Forsee, W. T. (1990) Calcium ion activation of rabbit liver alpha 1,2-mannosidase. *J. Biol. Chem. 265*, 2546−2549.
(30) Kiick, D. M., and Cleland, W. W. (1989) Steady-state kinetic studies of the metal ion-dependent decarboxylation of oxalacetate catalyzed by pyruvate kinase. *Arch. Biochem. Biophys. 270*, 647−654.